CLEO

CONFERENCE ON LASERS AND ELECTRO-OPTICS

25–29 APRIL 1988

Anaheim, California

while the sensing channel operates at 0.633 μm. The value of the normalized frequency at 0.633 μm is more than 2.405 so that a few higher-order modes can propagate at this wavelength in the core region.

Our experimental setup is schematically illustrated in Fig. 1. The beams from both the He–Ne laser and the semiconductor laser (central wavelength: 1307 nm) are injected into a 1.8-km long single-mode (at 1.3-μm) optical fiber through a single-mode power combiner. At the output end, the laser beams are spectrally separated by the 1.3-μm/0.633-μm WDM coupler. The light coupled out from the 1.3-μm channel is detected by an InGaAs detector and serves as the communication channel of the system. The light coupled out from the 0.633-μm channel is allowed to diverge into a speckle pattern in which a small-area Si-PIN photodetector is used to detect intensity fluctuations. This forms the sensing channel of the system.

Figure 2 (Fig. 3) shows simultaneously the communication signal and the sensing signal when the optical fiber is unperturbed (perturbed). The disturbance comes from a 2.77-kHz sound wave driving a speaker which slightly vibrates a coiled section about a 40-cm length of optical fiber. These figures demonstrate that the system is capable of sensing a disturbance, and, as can be seen, there is no distortion in the communication signal when the sensing signal exits. We have systematically studied the influence of fiber disturbance on communication quality by changing the frequency of the sound wave below, at, and above the modulation frequency of the communication signal. These experimental results reveal that our system can simultaneously function as a communicator and sensor and that no deterioration of the communication signal occurs.

Potential uses are also discussed.

(Poster paper)

1. R. Kist, in *Technical Digest, Fourth International Conference on Optical Fiber Sensors*, Tokyo (1986), p. 9.
2. C. Y. Leung, C. H. Huang, and I. F. Chang, Proc. Soc. Photo-Opt. Instrum. Eng. **838** (1987).

THM45 Interferometric dispersion measurements on small guided-wave structures

B. L. DANIELSON, C. D. WHITTENBERG, U.S. National Bureau of Standards, Electromagnetic Technology Division, 325 Broadway, Boulder, CO 80303.

Recent correlation–reflectometry techniques have demonstrated that loss in serial microoptic systems can be tracked with a spatial resolution of the order of a few micrometers.[1,2] We show here that the dispersion properties of individual components in these systems can also be measured from their reflection signatures. The method is based on Fourier transformation of the interferograms, as discussed by Bomberger and Burke.[3] To illustrate the technique, we measured the dispersion in a 23-mm sample of single-mode fiber in the scanning Michelson interferometer of Fig. 1. The time-domain sweep is done with a PZT and cat's-eye reflector and yields the signatures shown in Fig. 2. For the case of negligible transmission loss and balanced control arms, the transform of the cross-correlation interferogram gives a modulus that represents the source frequency spectrum and an argument representing the phase of the frequency components. The phase function can be expanded about the frequency at peak intensity as

$$\phi(\nu) = \phi(\nu_0 + \phi'(\nu_0)(\nu - \nu_0) + \frac{1}{2}\phi''(\nu_0)(\nu - \nu_0)^2 + \frac{1}{3!}\phi'''(\nu_0)(\nu - \nu_0)^3 + \ldots . \quad (1)$$

With a suitable choice of origin in the time domain, the second term in the expansion is zero. The third- and higher-order terms contain the dispersion information. The first-order dispersion in a transmission path x_0 is

$$D(\nu_0) = -\frac{\nu_0^2}{2\pi x_0 c}\phi''(\nu_0). \quad (2)$$

Results for our test lightguide are illustrated in Fig. 3. The phase with no sample in the reference arm is negligible in this case. A 1024-point FFT and Eq. (2) produce the values of $D = 19 \pm 1$ ps/km nm. The uncertainties quoted here are one-sigma values of the precision for repeated measurements and indicate the level of system noise. The slope of the dispersion can be estimated from the third-order derivative of $\phi(\nu)$ and has a magnitude of 0.13 ± 0.16 ps/km nm^2.

The presence of first-order dispersion implies a chirp in the time-domain signature. This effect can be observed in the experimental data.

The value of D obtained by Fourier transformation may be compared to the estimate derived from the broadening of the envelope of the interferogram. From the results of Shibata and co-workers[4] we can infer that for constant D and a Gaussian spectrum (only approximately true here), the envelope of the cross-correlation interferogram is also Gaussian and broadens according to the square root of the sum-of-squares rule that is usually associated with optical pulses. From this analysis D is $\sim$15 ps/km nm. Dispersion values obtained from Fourier analysis of the signature are, potentially at least, the more accurate of the two estimates.

While the transform method has some limitations when compared to the more conventional time-delay interferometric approach used for fibers,[5] it is attractive for the signature analysis of cascaded optical elements using coherence-domain reflectometry. **(Poster paper)**

1. B. L. Danielson and C. D. Whittenberg, Appl. Opt. **26**, 2836 (1987).
2. R. C. Youngquist, S. Carr, and D. E. N. Davies, Opt. Lett. **12**, 158 (1987).
3. W. D. Bomberger and J. J. Burke, Electron. Lett. **17**, 495 (1981).
4. M. T. Shibata, T. Nakashima, and S. Seikai, J. Opt. Soc. Am. A **4**, 494 (1987).
5. W. B. Gardner, Proc. Soc. Photo-Opt. Instrum. Eng. **559**, 18 (1985).

THM46 Continuous-wave tunable and Q-switched operation at 938 nm of a diode-laser-pumped Nd^{3+}-doped fiber laser

L. REEKIE, I. M. JAUNCEY, S. B. POOLE, D. N. PAYNE, U. Southampton, Dept. Electronics & Computer Science, Optical Fibre Group, Southampton, SO9 5NH, U.K.

Fiber lasers have been shown to offer a number of advantages over conventional crystal lasers operating in the near-IR region. The small mode size in the single-mode fiber enables high pump intensities to be relatively easily achieved without associated thermal problems. In addition, cw GaAlAs diode lasers have provided convenient pump sources for fiber lasers, and efficient operation at 1.09 (Ref. 1) and 1.55 μm (Ref. 2) has been demonstrated.

Room-temperature cw oscillation on the $^4F_{3/2}$–$^4I_{9/2}$ transition has been reported previously using a Nd^{3+}-doped single-mode fiber laser pumped by either a cw rhodamine 6G dye laser[3] or a diode laser.[4,5] Also, miniature Nd:YAG lasers operating at 946 nm have been demonstrated, pumped by a rhodamine 6G dye laser or a GaAlAs diode laser.[6] Here we report Q-switched and tunable operation of a diode laser-pumped Nd^{3+}-doped single-mode fiber laser operating on the three-level $^4F_{3/2}$–$^4I_{9/2}$ transition at 938 nm.

The experimental configuration of this laser has been described previously.[4] A Sharp LT015 GaAlAS laser diode operating at 823 nm was employed as the pump source. The fiber was characterized by a Nd^{3+} ion concentration of 1200 ppm, a core diameter of 3.4 μm, and a cutoff wavelength of 920 nm. The equivalent step-index N.A. of the fiber was 0.21. The input mirror was chosen to have a high transmission ($T = 85\%$) at the pump wavelength and high reflectivity ($R > 99\%$) at 936 nm, the lasing wavelength. To suppress the buildup of amplified spontaneity at 1.09 μm the input mirror reflectivity was low ($R = 3\%$) at this wavelength. The output mirror had a reflectivity of 57% at 936 nm and 40% at 1.09 μm. No attempt was made to optimize the output coupling.

The cw lasing characteristic obtained is shown in Fig. 1. The slope efficiency was 37% with a maximum output power of 3 mW and a laser threshold of 1.9-mW absorbed pump power. To avoid unwanted residual absorption of the three-level 938-nm emission it was necessary to determine the optimum fiber length. Additionally, if the fiber length was too short, output power was due to insufficient absorption of the pump light. Maximum output power and slope efficiency were obtained for a fiber length of 160 cm (Fig. 2).

Tunable operation was achieved by introducing an intracavity objective and replacing the output mirror with a bulk diffraction grating. The grating had 600 lines mm^{-1} and was blazed at 1 μm. Rotation of the grating enabled tuning of the laser to be achieved. An intracavity pellicle was inserted to couple out the output. The threshold for laser action in this configuration was 6.5 mW absorbed. At an absorbed pump power of 15 mW a tuning range of 40 nm was achieved, as shown in Fig. 3. The maximum output power at 936 nm was 0.2 mW.

Q-switching of this device has also been achieved by inserting an acoustooptic modulator into the cavity. Peak pulse power obtained to date has been limited to $\sim$1 W by the cavity configuration used. However, it is anticipated that powers in excess of 10 W will be readily achievable by simple modification of the cavity.

(Poster paper)

1. I. M. Jauncey, J. T. Lin, L. Reekie, and R. J. Mears, "An Efficient Diode-Pumped CW and Q-switched Single-Mode Fibre Laser," Electron. Lett. **22**, 198 (1986).
2. L. Reekie, I. M. Jauncey, S. B. Poole, and D. N. Payne, "Diode-Laser Pumped Operation of an Er^{3+}-Doped Single-Mode Fibre Laser," Electron. Lett. **22**, 159 (1986).
3. I. P. Alcock, A. I. Ferguson, D. C. Hanna, and A. C. Tropper, "Continuous-Wave Oscillation of a Monomode Neodymium-Doped Fibre Laser at 0.9 μm on the $^4F_{3/2}$–$^4I_{9/2}$ Transition," Opt. Commun. **58**, 405 (1986).
4. L. Reekie, I. M. Jauncey, S. B. Poole, and D. N. Payne, "Diode-Laser Pumped Nd^{3+}-Doped Fibre Laser Operating at 938 nm," Electron. Lett. **23**, 884 (1987).
5. H. Po, F. Hakimi, R. J. Mansfield, R. P. Tumminelli, B. C. McCollum, and E. Snitzer, "Neodymi-

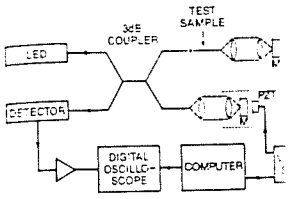

THM45 Fig. 1. Block diagram of the sc interferometer. The LED emission spec centered at 1550 nm and has a FWHM of 7

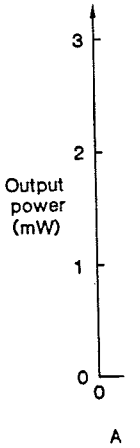

THM46 Fig. 1. laser operating a

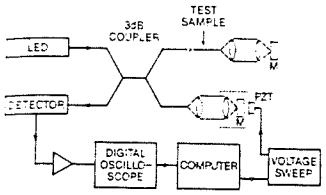

THM45 Fig. 1. Block diagram of the scanning interferometer. The LED emission spectrum is centered at 1550 nm and has a FWHM of 140 nm.

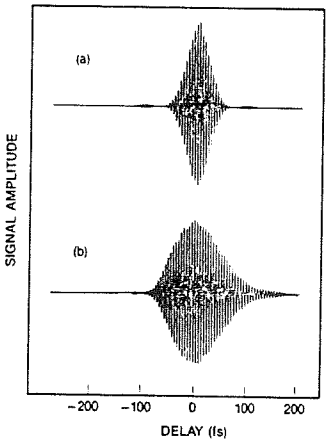

THM45 Fig. 2. Autocorrelation (a) and cross-correlation (b) interferograms for the fiber sample.

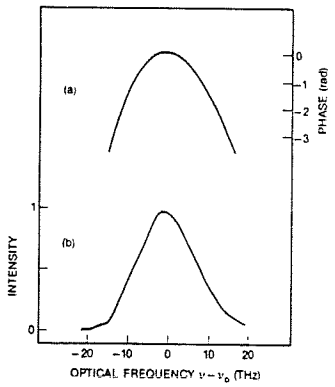

THM45 Fig. 3. Phase (a) and relative spectral intensity (b) from Fourier transformation of the cross-correlation inteferogram.

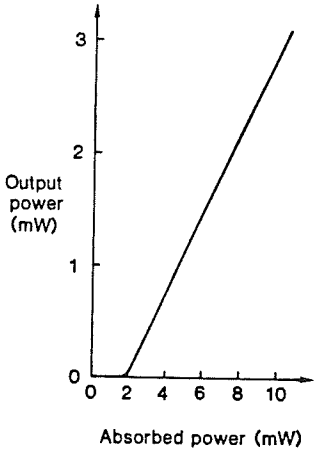

THM46 Fig. 1. Lasing characteristic of a fiber laser operating at 938 nm.

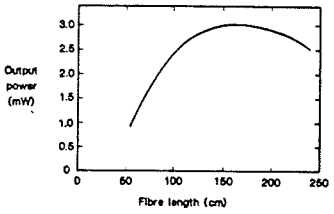

THM46 Fig. 2. Maximum output power obtainable as a function of fiber length.

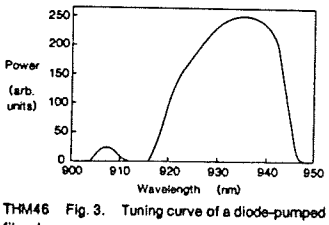

THM46 Fig. 3. Tuning curve of a diode-pumped fiber laser.

Poster Thursday